Fluorescent Probes

DOI: 10.1002/anie.201202533

A Tunable Ratiometric pH Sensor Based on Carbon Nanodots for the Quantitative Measurement of the Intracellular pH of Whole Cells**

Wen Shi, Xiaohua Li, and Huimin Ma**

Intracellular pH modulates the function of many organelles and plays a pivotal role in cell metabolism processes, such as the proliferation and apoptosis.[1] Measuring pH distribution and fluctuation with high temporal–spatial resolution in living cells is thus essential for advancing our understanding of cell biology. Towards this end, great efforts have been made to develop ratiometric fluorescent pH sensors, because such sensors can avoid the influence of several variants, such as concentration and optical path length, and have been proved to be an effective way to accurately quantify the pH values in cells and even in organelles.[2] Small molecular fluorescent probes as well as fluorescent proteins have been widely used for intracellular pH detection. Recently, nanoparticle-based ratiometric pH sensors have attracted more and more attention owing to their remarkable advantages, the most important of these being that it is easy to simultaneously assemble diverse dyes (usually pH-sensitive and pH-insensitive) on the same nanoparticle to acquire ratiometric fluorescent sensors with tunable pH response range.[3]

A number of fluorescent nanosensors, based on silicon, polymers, or quantum dots, have been elegantly designed to quantify intracellular pH.[3] However, most of them only report the pH value of endosomes or lysosomes in cells instead of the whole intracellular pH map, including the cytoplasm and nucleus. The possible reason for this phenomenon might be that the large size or limited biocompatibility of the nanosensors leads to their localized distribution. Thus, smaller size and more biocompatible materials would be desirable.

The newly emerging carbon nanodots (CDs), the latest form of carbon nanomaterials,[4] possess such properties and may be considered as a favorable candidate. Specifically, their good biocompatibility has led to their successful use in imaging living cells and delivering drugs,[5] and their small sizes (usually having a diameter less than 10 nm) may facilitate the diffusion in cells. These superior characteristics of CDs, together with their facile preparation, make them a promising material for fluorescent pH sensors. However, such an attempt has not been reported to our knowledge. Herein, we describe the first example of CD-based tunable ratiometric fluorescent pH sensor by which the intracellular pH pattern of HeLa cells is quantitatively obtained. Moreover, the intracellular pH fluctuation caused by different redox species is also studied with the nanosensor.

The CD-based fluorescent pH sensor was fabricated as depicted in Scheme 1. First, amino-coated CDs were prepared by heating citric acid in glycerol at 220 °C for 3 h under argon in the presence of 4,7,10-trioxa-1,13-tridecanediamine (TTDDA; as a surface coating agent). The amino-coated CDs were then treated with different molar ratios (1:1–1:30) of pH-sensitive fluoresceinisothiocyanate (FITC) to pH-insensitive rhodamine B isothiocyanate (RBITC), yielding the dual-labeled CDs (DLCDs), which were finally purified by thorough dialysis and gel chromatographic separation. The red solution of DLCDs that was obtained, which is stable for at least six months, can be used directly, or lyophilized as a red solid, which can be easily redispersed in water. The diameter of DLCDs by transmission electron microscopy measurement is approximately 5 nm (Supporting Information, Figure S1), and its average hydrodynamic diameter in water is about 7 nm from dynamic light scattering analysis (Supporting Information, Figure S2).

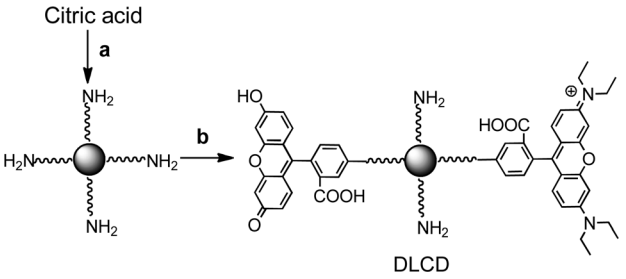

Scheme 1. Preparation of dual-labeled carbon nanodots (DLCDs). a) TTDDA, 220 °C, 3 h; b) FITC, RBITC, room temperature, overnight. See text for details.

The fluorescence emission spectra of DLCDs were examined in Na_2HPO_4/NaH_2PO_4 buffer solution at various pH values. Ratiometric fluorescent pH sensors are usually utilized in dual excitation mode,[2,3] which suffers from some drawbacks, such as complex equipment and operation and poor time resolution. Therefore, in this work a single excitation mode (at 488 nm) was chosen. As an optimized example (see below), the DLCDs prepared with a molar ratio of 1:10 FITC/RBITC show a distinct fluorescent response to pH. As depicted in Figure 1 a, the increase of pH raises the fluorescence (515 nm) of fluorescein dramatically, while that

[*] Dr. W. Shi, Prof. Dr. X. H. Li, Prof. Dr. H. M. Ma
Beijing National Laboratory for Molecular Sciences
Key Laboratory of Analytical Chemistry for Living Biosystems
Institute of Chemistry, Chinese Academy of Sciences
Beijing 100190 (China)
E-mail: mahm@iccas.ac.cn

[**] This work is supported by grants from the NSF of China (Nos. 21105104, 20935005, and 20905070), National Basic Research Program of China (Nos. 2011CB935800 and 2010CB933502), and the Chinese Academy of Science (KJCX2-EW-N06-01).

Supporting information for this article is available on the WWW under http://dx.doi.org/10.1002/anie.201202533.

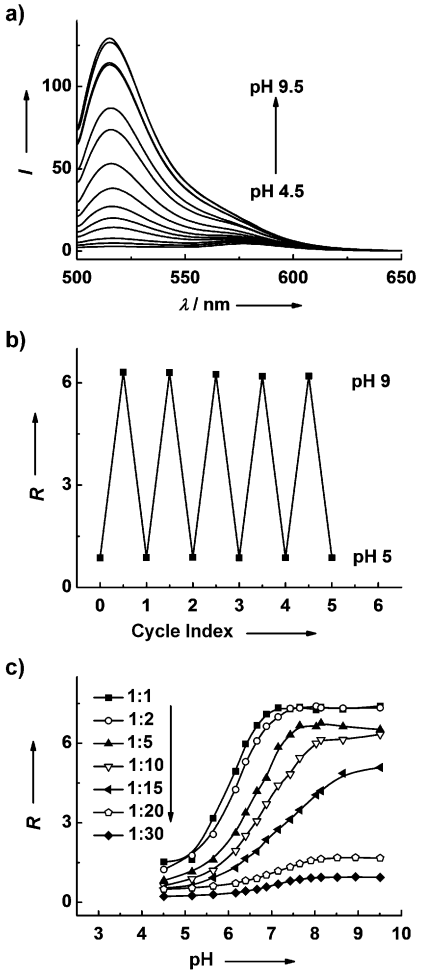

Figure 1. a) Fluorescence emission spectra of DLCDs (60 μg mL^{-1}) in 0.2 M Na_2HPO_4/NaH_2PO_4 buffer at various pH values. b) pH reversibility study of DLCDs between pH 5 and 9. c) Plots of *R* versus pH values for DLCDs prepared with different molar feed ratios from 1:1 to 1:30 (FITC/RBITC). *R* is the ratio (I_{515}/I_{575}) of the fluorescence intensity of DLCDs at 515 nm and 575 nm; $\lambda_{ex} = 488$ nm.

(575 nm) of rhodamine B is increased little. The fluorescence intensity ratio *R* of fluorescein at 515 nm and rhodamine B at 575 nm increases with the increase in pH. Most notably, the pH sensor displays an excellent reversibility between pH 5 and pH 9 (Figure 1b).

The molar feed ratio of FITC to RBITC is a critical factor for the pH response range of DLCDs. As shown in Figure 1c, different feed ratios from 1:1 to 1:30 FITC/RBITC make the pH-sensitive range of the nanosensor tunable from pH 5.2 to 8.5, which can cover most of the physiological pH ranges. However, a higher content of RBITC would decrease the sensitivity of the sensor. Considering the intracellular pH fluctuation range, DLCDs with a molar feed ratio of 1:10 were employed in the present work unless otherwise noted, because its optimized pH-sensitive range is about pH 5.2–8.2. In this case, the amounts of FITC and RBITC conjugated to per gram of the CDs are calculated to be about 53 mg and 419 mg, respectively, based on the additivity of absorbance from each component (Supporting Information, Figure S3).

The influence of intracellular species, such as ions, saccharides and proteins, on the quantitative pH determination were investigated, revealing that these species over their physiological concentrations exhibit negligible effect (Supporting Information, Figure S4). Furthermore, to explore the intracellular pH fluctuations associated with oxidative stress, the effects of redox substances, including H_2O_2, ClO^-, reduced glutathione (GSH), GSH inhibitor N-ethyl maleimide (NEM),[6] and GSH precursor *N*-acytelcysteine (NAC),[7] were examined in phosphate buffer saline (PBS, pH 7.4). It is found that these substances scarcely affect the ratiometric fluorescent signal of DLCDs (Supporting Information, Figure S5); that is, interference from their redox and/or acid–base properties may be neglected.

A standard MTT assay (MTT = 3-(4,5-dimethylthiazol-2-yl)-2,5-diphenyl-tetrazolium bromide)[8] showed that cell viability was not significantly changed upon treatment with DLCDs for 24 h (Supporting Information, Figure S6), clearly indicating the low cytotoxicity and good biocompatibility of the CD-based sensor.

To demonstrate the applicability of DLCDs to quantifying intracellular pH, the intracellular calibration experiment was first made in HeLa cells with H^+/K^+ ionophore nigericin, which is a standard approach for homogenizing the pH of cells and culture medium.[9] As shown in Figure 2, the fluorescence from the FITC channel (green pseudocolor) in cells increases with pH, whereas that from the RBITC channel (red pseudocolor) hardly alters. The ratio channel, obtained based on the above two channels, displays a characteristic pH-dependent signal (the fourth row in Figure 2), which generates a good linear calibration curve in the pH range from 6.0 to 8.0 (Figure 3a). On the basis of this curve, the averaged intracellular pH value of intact HeLa cells (Figure 3b; Supporting Information, Figure S7) is determined to be 7.4 ± 0.2. It is noted that the difference of the ratio signals between cytoplasm and nucleus is not significant, implying that these two regions have a similar pH environment. Moreover, the applicability of DLCDs was further demonstrated by measuring the intracellular pH of MCF-7 cells (Supporting Information, Figure S8), and a lower pH value (7.2 ± 0.2) than that of HeLa cells was observed. To verify the validity of DLCDs, SNARF-1 (a commercial available pH probe) was used to determine the intracellular pH values of HeLa and MCF-7 cells. The results obtained from SNARF-1 accord well with those from DLCDs (Supporting Information, Figure S9).

Detailed fluorescence imaging analysis (Supporting Information, Figure S7) shows that DLCDs can be distributed in the whole HeLa cells rather than the specific organelles like endosomes or lysosomes, which is quite different from that of the other nanoparticle-based sensors such as silicon, polymers or semiconductor quantum dots. Importantly, the unnoticeable difference of fluorescence intensity between cytoplasm and nucleus indicates the good dispersibility of DLCDs in cells. This feature of DLCDs may result from the better biocompatibility and smaller size of CDs. Similar intracellular distribution patterns in both cytoplasm and nucleus have been observed for other carbon nanomaterials, such as carbon nanotubes[10] and graphene.[11] Interestingly, in the RBITC channel (Supporting Information, Figure S7, second row) we

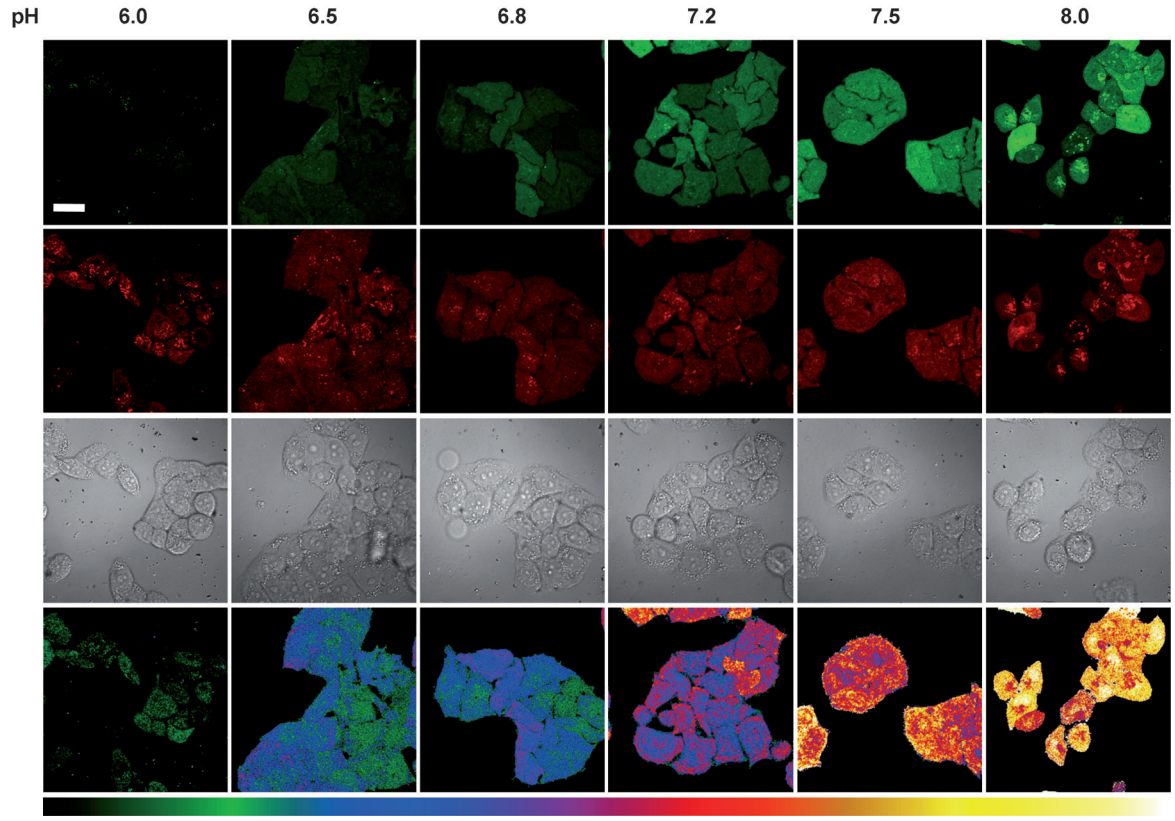

Figure 2. Fluorescent images of HeLa cells clamped at pH 6.0, 6.5, 6.8, 7.2, 7.5, and 8.0, respectively. The images of the first row (FITC channel) and second row (RBITC channel) were collected in the ranges of 510–550 nm and 570–610 nm, respectively. The third row shows the corresponding differential interference contrast images. The images of the fourth row (the ratio channel) were generated by Olympus software (FV10-ASW); the bottom color strip represents the pseudocolor change with pH. Scale bar, 20 μm.

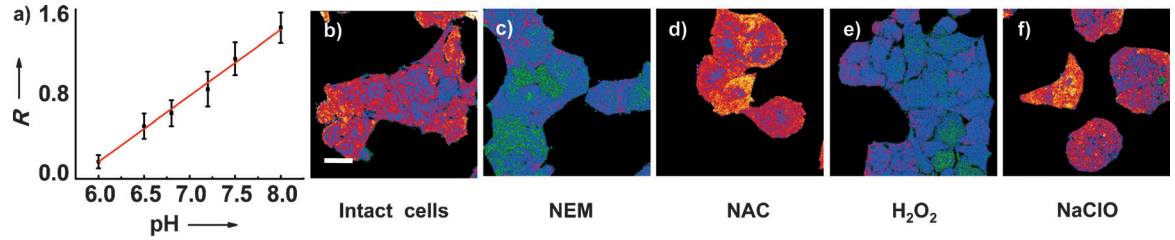

Figure 3. a) Intracellular pH calibration curve of DLCDs. *R* indicates the pseudo ratio generated by Olympus software (FV10-ASW). b)–f) Ratiometric images of DLCD-loaded HeLa cells in PBS (pH 7.4): b) intact cells, and cells treated with c) 1 mM NEM, d) 1 mM NAC, e) 100 μM H_2O_2, or f) 100 μM NaClO for 1 h. Scale bar: 20 μm. See the Supporting Information, Figure S7, for more details.

can see bright discrete spots, which correspond to the acidic speckles in the ratio channel (Supporting Information, Figure S7, fourth row). This phenomenon might be attributed to the slight accumulation of DLCDs in endosomes or lysosomes, which however does not disturb the measurement of the whole intracellular pH.

Different redox substances were applied to HeLa cells to explore the relationship between intracellular pH fluctuations and oxidative stress. First, NEM (GSH inhibitor) or NAC (GSH precursor) was incubated with HeLa cells to regulate the intracellular GSH level. As shown in Figure 3c, the depletion of GSH by NEM decreases the intracellular pH to 6.9 ± 0.3. The reason for this acidification is unclear, but a possible explanation may be that the decrease of GSH may affect the function of the Na^+/H^+ antiporter.[12] However, the upregulation of GSH by NAC has no considerable effect on the intracellular pH (Figure 3d), indicating that GSH over the normal concentration may not cause a noticeable change of the intracellular acidic substances.

Similarly, H_2O_2 can acidify HeLa cells to pH 7.0 ± 0.2 (Figure 3e), which has been ascribed to the generation of acidic substances (for example, phosphoric acid) caused by hydroxyl radicals (Fenton reaction) from H_2O_2.[13] Interestingly, low intracellular pH was not observed when HeLa cells were treated with NaClO (Figure 3f), suggesting that the elevated level of ClO^- cannot increase greatly the intracellular acidic substances under the present conditions. This behavior of ClO^-, which is quite different from that of H_2O_2,

has not been reported yet to the best of our knowledge. Moreover, all these trends of intracellular pH changes in the presence of redox substances are supported by a comparative study with SNARF-1 (Supporting Information, Figure S10), confirming the validity of our nanosensor.

In conclusion, a tunable ratiometric fluorescent pH nanosensor has been developed by incorporating FITC and RBITC to carbon nanodots, whose noticeable feature is the facile adjustment of pH response range compared to most of the known pH sensors. Cell imaging studies have demonstrated its good biocompatibility and intracellular dispersibility. Quantitative determinations of intracellular pH of intact HeLa cells and the pH fluctuations associated with oxidative stress have been successfully performed with our nanosensor. The decrease of intracellular GSH leads to the acidification of cells, but GSH above the normal level has no obvious effect on the intracellular pH. Moreover, elevated ClO^- does not decrease the intracellular pH as H_2O_2 does. The detailed mechanisms for these phenomena need to be studied in the future. However, the present study leads to an interesting observation that the disturbance of oxidative stress usually decreases rather than increases the intracellular pH (unidirectional change), which is further supported by the measurements with SNARF-1. More notably, this work clearly shows that CDs can serve as a promising platform for constructing practical fluorescent nanosensors, and the proposed DLCD sensor may have a great potential for quantitatively monitoring the intracellular pH fluctuations under different stimuli.

Received: April 1, 2012
Published online: May 29, 2012

Keywords: carbon nanodots · fluorescent probes · intracellular pH · ratiometric imaging · sensors

[1] a) D. Pérez-Sala, D. Collado-Escobar, F. Mollinedo, *J. Biol. Chem.* **1995**, *270*, 6235 – 6242; b) R. A. Gottlieb, J. Nordberg, E. Skowronski, B. M. Babior, *Proc. Natl. Acad. Sci. USA* **1996**, *93*, 654 – 658; c) L. D. Shrode, H. Tapper, S. Grinstein, *J. Bioenerg. Biomembr.* **1997**, *29*, 393 – 399.

[2] a) J. Y. Han, K. Burgess, *Chem. Rev.* **2010**, *110*, 2709 – 2728, and references therein; b) G. R. Bright, G. W. Fisher, J. Rogowska, D. L. Taylor, *J. Cell Biol.* **1987**, *104*, 1019 – 1033; c) K. A. Giuliano, R. J. Gillies, *Anal. Biochem.* **1987**, *167*, 362 – 371; d) C. L. Slayman, V. V. Moussatos, W. W. Webb, *J. Exp. Biol.* **1994**, *196*, 419 – 438; e) T. Myochin, K. Kiyose, K. Hanaoka, H. Kojima, T. Terai, T. Nagano, *J. Am. Chem. Soc.* **2011**, *133*, 3401 – 3409; f) B. Tang, F. Yu, P. Li, L. Tong, X. Duan, T. Xie, X. Wang, *J. Am. Chem. Soc.* **2009**, *131*, 3016 – 3023; g) J. Y. Han, A. Loudet, R. Barhoumi, R. C. Burghardt, K. Burgess, *J. Am. Chem. Soc.* **2009**, *131*, 1642 – 1643; h) E. Nakata, Y. Yukimachi, Y. Nazumi, Y. Uto, H. Maezawa, T. Hashimoto, Y. Okamoto, H. Hori, *Chem. Commun.* **2010**, *46*, 3526 – 3528; i) J. Llopis, J. M. McCaffery, A. Miyawaki, M. G. Farquhar, R. Y. Tsien, *Proc. Natl. Acad. Sci. USA* **1998**, *95*, 6803 – 6808; j) R. Bizzarri, C. Arcangeli, D. Arosio, F. Ricci, P. Faraci, F. Cardarelli, F. Beltram, *Biophys. J.* **2006**, *90*, 3300 – 3314; k) M. Tantama, Y. P. Hung, G. Yellen, *J. Am. Chem. Soc.* **2011**, *133*, 10034 – 10037; l) M. H. Su, Y. Liu, H. M. Ma, Q. L. Ma, Z. H. Wang, J. L. Yang, M. X. Wang, *Chem. Commun.* **2001**, 960 – 961.

[3] a) H. S. Peng, J. A. Stolwijk, L. N. Sun, J. Wegener, O. S. Wolfbeis, *Angew. Chem.* **2010**, *122*, 4342 – 4345; *Angew. Chem. Int. Ed.* **2010**, *49*, 4246 – 4249; b) L. Albertazzi, B. Storti, L. Marchetti, F. Beltram, *J. Am. Chem. Soc.* **2010**, *132*, 18158 – 18167; c) R. V. Benjaminsen, H. Sun, J. R. Henriksen, N. M. Christensen, K. Almdal, T. L. Andresen, *Acs Nano* **2011**, *5*, 5864 – 5873; d) Y. H. Chan, C. Wu, F. Ye, Y. Jin, P. B. Smith, D. T. Chiu, *Anal. Chem.* **2011**, *83*, 1448 – 1455; e) S. Q. Wu, Z. Li, J. H. Han, S. F. Han, *Chem. Commun.* **2011**, *47*, 11276 – 11278; f) H. Sun, K. Almdal, T. L. Andresen, *Chem. Commun.* **2011**, *47*, 5268 – 5270; g) K. Zhou, Y. Wang, X. Huang, K. Luby-Phelps, B. D. Sumer, J. Gao, *Angew. Chem.* **2011**, *123*, 6233 – 6238; *Angew. Chem. Int. Ed.* **2011**, *50*, 6109 – 6114; h) J. Lei, L. Wang, J. Zhang, *Chem. Commun.* **2010**, *46*, 8445 – 8447.

[4] a) S. N. Baker, G. A. Baker, *Angew. Chem.* **2010**, *122*, 6876 – 6896; *Angew. Chem. Int. Ed.* **2010**, *49*, 6726 – 6744; b) H. Peng, J. Travas-Sejdic, *Chem. Mater.* **2009**, *21*, 5563 – 5565; c) F. Wang, S. Pang, L. Wang, Q. Li, M. Kreiter, C. Y. Liu, *Chem. Mater.* **2010**, *22*, 4528 – 4530; d) H. Liu, T. Ye, C. Mao, *Angew. Chem.* **2007**, *119*, 6593 – 6595; *Angew. Chem. Int. Ed.* **2007**, *46*, 6473 – 6475; e) X. Wang, L. Cao, S. T. Yang, F. Lu, M. J. Meziani, L. Tian, K. W. Sun, M. A. Bloodgood, Y. P. Sun, *Angew. Chem.* **2010**, *122*, 5438 – 5442; *Angew. Chem. Int. Ed.* **2010**, *49*, 5310 – 5314; f) R. Liu, D. Wu, S. Liu, K. Koynov, W. Knoll, Q. Li, *Angew. Chem.* **2009**, *121*, 4668 – 4671; *Angew. Chem. Int. Ed.* **2009**, *48*, 4598 – 4601; g) T. N. Hoheisel, S. Schrettl, R. Szilluweit, H. Frauenrath, *Angew. Chem.* **2010**, *122*, 6644 – 6664; *Angew. Chem. Int. Ed.* **2010**, *49*, 6496 – 6515; h) H. Li, X. He, Z. Kang, H. Huang, Y. Liu, J. Liu, S. Lian, C. H. A. Tsang, X. Yang, S. T. Lee, *Angew. Chem.* **2010**, *122*, 4532 – 4536; *Angew. Chem. Int. Ed.* **2010**, *49*, 4430 – 4434; i) K. Y. Niu, H. M. Zheng, Z. Q. Li, J. Yang, J. Sun, X. W. Du, *Angew. Chem.* **2011**, *123*, 4185 – 4188; *Angew. Chem. Int. Ed.* **2011**, *50*, 4099 – 4102; j) L. Zhao, T. Takimoto, M. Ito, N. Kitagawa, T. Kimura, N. Komatsu, *Angew. Chem.* **2011**, *123*, 1424 – 1428; *Angew. Chem. Int. Ed.* **2011**, *50*, 1388 – 1392.

[5] a) L. Cao, X. Wang, M. J. Meziani, F. Lu, H. Wang, P. G. Luo, Y. Lin, B. A. Harruff, L. M. Veca, D. Murray, S. Y. Xie, Y. P. Sun, *J. Am. Chem. Soc.* **2007**, *129*, 11318 – 11319; b) S. T. Yang, X. Wang, H. F. Wang, F. S. Lu, P. G. Luo, L. Cao, M. J. Meziani, J. H. Liu, Y. F. Liu, M. Chen, Y. P. Huang, Y. P. Sun, *J. Phys. Chem. C* **2009**, *113*, 18110 – 18114; c) Q. Li, T. Y. Ohulchanskyy, R. Liu, K. Koynov, D. Wu, A. Best, R. Kumar, A. Bonoiu, P. N. Prasad, *J. Phys. Chem. C* **2010**, *114*, 12062 – 12068; d) A. H. Faraji, P. Wipf, *Bioorg. Med. Chem.* **2009**, *17*, 2950 – 2962; e) S. M. Janib, A. S. Moses, J. A. MacKay, *Adv. Drug Delivery Rev.* **2010**, *62*, 1052 – 1063; f) Y. K. Tzeng, O. Faklaris, B. M. Chang, Y. Kuo, J. H. Hsu, H. C. Chang, *Angew. Chem.* **2011**, *123*, 2310 – 2313; *Angew. Chem. Int. Ed.* **2011**, *50*, 2262 – 2265.

[6] a) C. R. Yellaturu, M. Bhanoori, I. Neeli, G. N. Rao, *J. Biol. Chem.* **2002**, *277*, 40148 – 40155; b) J. X. Lu, Y. C. Song, W. Shi, X. H. Li, H. M. Ma, *Sens. Actuators B* **2012**, *161*, 615 – 620.

[7] R. Ruffmann, A. Wendel, *J. Mol. Med.* **1991**, *69*, 857 – 862.

[8] M. Tim, *J. Immunol. Methods* **1983**, *65*, 55 – 63.

[9] M. Tafani, J. A. Cohn, N. O. Karpinich, R. J. Rothman, M. A. Russo, J. L. Farber, *J. Biol. Chem.* **2002**, *277*, 49569 – 49576.

[10] a) A. E. Porter, M. Gass, K. Muller, J. N. Skepper, P. A. Midgley, M. Welland, *Nat. Nanotechnol.* **2007**, *2*, 713 – 717; b) D. Pantarotto, J. Briand, M. Prato, A. Bianco, *Chem. Commun.* **2004**, 16 – 17.

[11] C. Peng, W. B. Hu, Y. T. Zhou, C. H. Fan, Q. Huang, *Small* **2010**, *6*, 1686 – 1692.

[12] M. R. Ciriolo, A. T. Palamara, S. Incerpi, E. Lafavia, M. C. Bue, P. DeVito, E. Garaci, G. Rotilio, *J. Biol. Chem.* **1997**, *272*, 2700 – 2708.

[13] K. L. Tsai, S. M. Wang, C. C. Chen, T. H. Fong, M. L. Wu, *J. Physiol.* **1997**, *502*, 161 – 174.

